'Modelling of Microshocks Associated With High-Voltage Equipment'

A. Gunatilake, Y. Ahmed, S. M. Rowland

IEEE Transactions on Power Delivery, Vol. 24, Issue 1, (2009): pages 202 - 207

Digital Object Identifier: 10.1109/TPWRD.2008.2005366

Modelling of Microshocks Associated with High Voltage Equipment

A. Gunatilake *Student Member, IEEE,* Y. *A*hmed, *Graduate Member, IEEE*
and S. M. Rowland, *Senior Member, IEEE*

***Abstract*— Bodies close to high voltage equipment may experience discharges to metallic objects at ground potential if they are not grounded themselves. A tool which is able to predict the occurrence of such events would provide considerable benefit to transmission network operators. In this study, models of microshocks are developed. Laboratory measurements coupling an HV overhead line to a simple model of a human body are compared to the predictions of a commercially available software package. The software, called CDEGS (Current Distribution, Electromagnetic Fields, Grounding and Soil Structure Analysis), is widely used in the power industry. The experimental measurement of the potential of the floating body is complex because of the high field in which it sits, and this is also discussed. The software is found to represent the measured data in the simple cases examined to within 10%, and is found to be satisfactory as a platform for further development.**

***Index Terms*—air gaps, gas discharges, high voltage techniques, software tools.**

I. Introduction

Microshocks is a term which has come to be used to describe electric discharges which result from a body which is at an elevated potential as a result of capacitive coupling to high voltage equipment[1]. Such discharges occur as the body approaches an earthed object. In practice such events are experienced mainly by linesmen. As a linesman's body is capacitively coupled to high voltage overhead lines, and if he is not earthed well, his potential will rise. If he comes close to an earthed object such as a tower, and the voltage between the object and his body is high enough, a discharge can arise between the linesman and the object. Unlike a static discharge, one or more such discharge can occur within every half cycle of the power frequency. An equivalent circuit is shown in Fig. 1. The capacitances depicted in Fig. 1 are distributed geometric capacitances. C_a represents the capacitance of the object or man to the conductors. In this case just one such conductor is shown. C_b represents the capacitance of the object to ground. This may be dominated by the tower or the ground plane. In the case of the object being a person, a capacitance C_s is used to represent the capacitance of the feet of the person to ground. This is determined by the footwear of the individual. In this case C_b represents the capacitance of the object to ground excluding the contribution of the feet C_s.

The voltage of the person in Fig. 1 will rise depending upon the values of C_a and C_b+C_s. If the potential of the man exceeds the breakdown voltage of a gap between himself and an earthed object, he will discharge and a spark will result. The current in the discharge arises from the energy stored on C_b and C_s, the flow of energy from the conductor is limited by the high impedance presented by the capacitive coupling to the high voltage source, C_a.

Linesmen working on high voltage equipment occasionally report tingling sensations in their finger tips. Often this is just an annoyance, but the levels can become such that work has to cease. One key issue for the management of this situation is that the phenomenon is not readily predictable in the field, and it can be a problem on one day and not another in an apparently identical situation.

The IEEE standard C95.6-2002 [2] specifies a maximum permissible exposure to power frequency electrical fields of 5 kV/m for the general public, and 20 kV/m in controlled working environments. Measurements suggest these latter limits are exceeded in some circumstances [3], [4]. The issue of microshocks is not known to present any long-term health issues [2]. Individual perception may be dependent on the individual person, and their skin condition. In addition the impedance of the body which is a complex issue in itself [5]-[9] will have an impact on the nature of discharges, and therefore perception and it has previously been shown that sensitivity varies between individuals [10], [11].

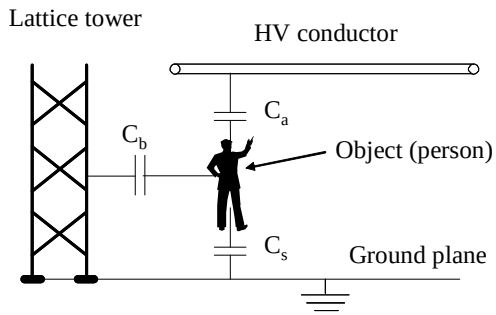

Fig. 1. Schematic of the electrical situation of the object.

This work was supported by National Grid.

S. M. Rowland, A. Gunatilake and Y. Ahmed, are all with The University of Manchester, Manchester, M60 1QD, UK.
(e-mail: s.rowland@manchester.ac.uk)

The mean perception level of current for men has been determined as 1.1 mA [6], although this value is very dependent on the nature of the experiment performed. The sensation at the perception threshold is mild and not unpleasant, and well below the values at which muscle control is lost, the lower 0.5 percentile values of which are 9 mA for men and 6 mA for women [6].

The purpose of the work presented here is to examine whether readily available software might be used to predict when fields are sufficiently high to lead to the occurrence of discharges which cause microshocks. Moreover software has been chosen which may allow extension of this work to predict the severity of the microshock experience. The work presented here does not address the psychological and physiological issues which control human perception of such discharges.

II. The Nature of Microshock Events

Previous analyses of the occurrence of discharges [3], and small-scale laboratory measurements [10] have described the apparent simplicity of the initiation condition for microshocks to occur. In the simplest of models the occurrence of a discharge can be represented by the closure of a switch in parallel to the capacitor C_b in Fig. 1. In a laboratory test using equivalent components it was found that such a spark partially discharges the capacitor from a initial value of around 1kV to about 500V, although this latter value depends upon skin condition [11], [12].

The schematic of Fig. 1 may be drawn as a lumped circuit diagram of Fig. 2. In this diagram C_a and C_b still represent distributed capacitances. The switch S_1 closing represents the existence of a discharge. The discharge resistance and the body impedance are all represented by R_d.

The work reported here is intended to show that software models are capable of predicting the voltage levels seen in practice, and also that the voltages at which discharges occur are consistent with expectations for small air gaps. For this reason we are not concerned with the complexities of R_d which determines the nature of the discharge itself.

If we consider a finger in close proximity to the tower, we note that the voltage at which discharges will occur will be a function of the gap length. In the voltage range concerned (around 1 kV) the gap length at breakdown in small (less than a few mm) and so in reality the finger is dynamically moving and the gap itself is not constant. On contact, when the gap is closed, no discharges will occur but an ac current will flow restricted by the impedance of C_a.

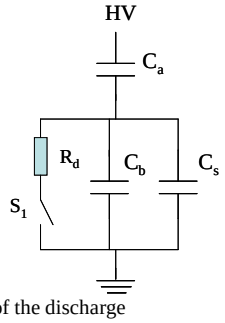

Fig. 2. Equivalent circuit of the discharge

In the laboratory, the voltage at which a gap breaks down can be measured. The circuit diagram of a typical test setup is shown in Fig. 3. The values of breakdown voltage obtained for metallic electrodes at variable separation are shown in Fig 4. In this case one electrode was planar and the other a cylinder of radius 6.25 mm, rounded off in a hemisphere. Both were made of brass and cleaned with nylon wool before each experiment. This cleaning process was sufficient because in these tests, discharges had insufficient energy to 'pit' the electrodes. The breakdown values shown Fig. 4 occur at the peak of the 50 Hz sine wave, and so a single breakdown event occurs per half cycle. The error associated with air gap length and point on wave voltage measurements were ±0.1 mm and ±0.5 kV respectively. By increasing the voltage for a given air gap a level can be reached whereby two discharges occur per half cycle. The voltage required for this depends upon the breakdown voltage for the air gap. Fig. 5 shows a measured breakdown pattern over a complete 50Hz cycle where two breakdowns occurred in the first half cycle.

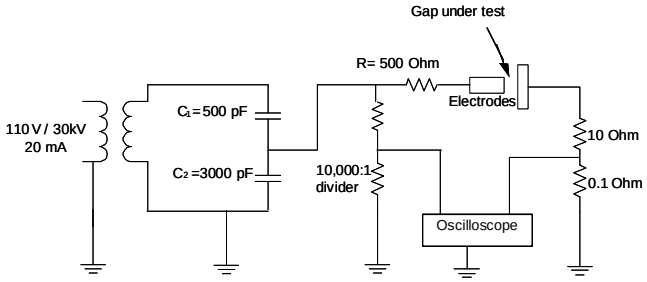

Fig. 3. Laboratory circuit used to generate discharges.

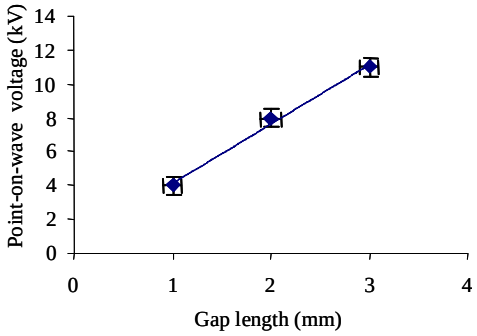

Fig 4. Variation of point-on-wave breakdown voltage with gap length.

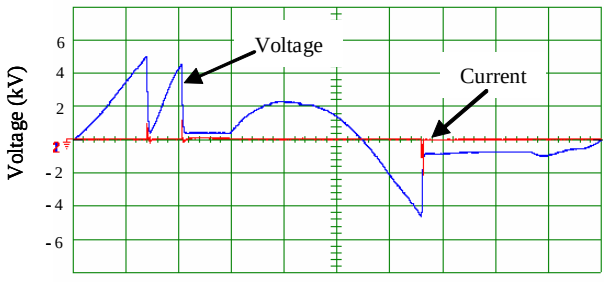

Fig. 5. The blue line shows the voltage across the gap. In the first half cycle two discharges occur. The red line indicates gap current.

If a discharge gap is fed directly from an ac power supply, the minimum voltage amplitude V_p^n required for n discharges per half cycle of the sinusoidal waveform can be shown to be given by:

$$V_p^{\,n} = \frac{V_b}{Sin\left[\frac{\pi}{2} - (n-1)\pi f\tau\right]} \qquad (1)$$

where V_b is the point-on-wave breakdown voltage for the gap, f is the power frequency and τ is the time for the voltage to recover between breakdown events within a cycle. This assumes a fixed recovery time, and if this is treated as the variable (1) can be used to predict the number of breakdowns per half cycle as a function of the recovery time as shown in Fig 6. This simple treatment shows that for a given voltage amplitude, the number of discharges increases in a non-linear fashion as the recovery time is reduced. For example, 4 discharges will occur per half cycle for τ = 3ms with a voltage amplitude of 6.4 x V_b, whereas if τ = 1ms a voltage amplitude of only 1.1 x V_b is required.

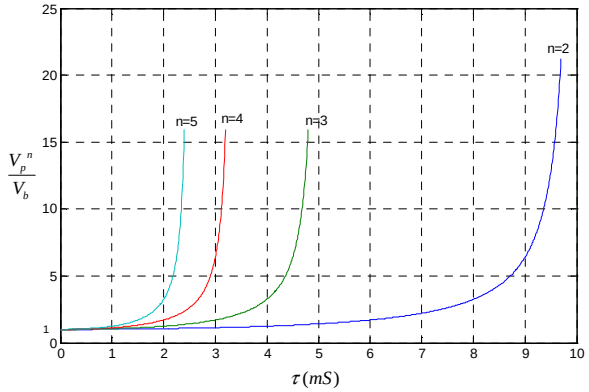

Fig. 6. The prediction of number of breakdowns, n, per half cycle as a function of recovery time, τ, and ratio of peak applied source voltage to the point-on-wave breakdown voltage.

The situation in the case of microshocks cannot be modeled in such a simplified way. In this case the charging current is fed through the capacitor C_a and the recharging time depends upon the rate of change of the voltage across C_a since this determines the charging current. Experimental values of peak sinusoidal voltage for multiple breakdowns with different air gap lengths are shown in Fig. 7.

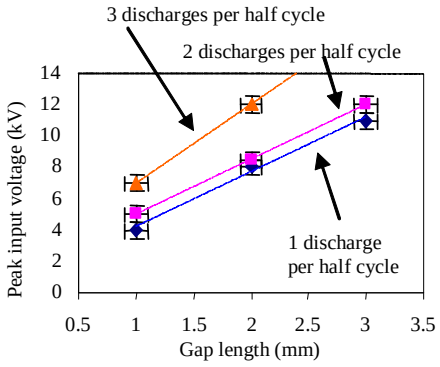

Fig 7. Variation of peak input voltage with number of breakdowns.

A simulation was built in PSCAD/EMTDC software with the components identified in Fig. 3. The air gap is modeled as a breaker which closes at a defined breakdown voltage and has a fixed value of arc resistance. The choice of resistance has a subtle impact on the results. When there is no arc, the air gap is represented by a 1pF capacitance. The switch is set to close when the point-on-wave reaches 4 kV. In this model the switch is closed for an arbitrary 1.7 µs and then re-opened, allowing multiple discharges per cycle. The predicted voltage waveform is shown in Fig. 8 for the voltage at the transformer secondary, Ea, the voltage across C_1, dV, the voltage across C_2, Eb, and at the HV electrode, Ec. For clarity the vertical scale has been increased by a factor of 5 for Eb and Ec. As expected Ea is the sum of dV and Eb. And Eb is close in value to Ec.

Increasing the value of the series resistor, from 500 Ω to 10 kΩ in the circuit of Fig. 3, results in the waveforms of Fig. 9. The principle difference is that the potential on the HV electrode, Eb, does not return to zero on discharge.

The experimental measurements, analytical predictions and PSCAD/EMTDC software are all consistent with the understanding of the cause of microshocks presented in this paper. However the use of circuit models assumes knowledge of equivalent component values such as C_1 and C_2 and clearly this is not always possible. This is the motivation for using a platform which can determine voltages using geometric information about the physical system, and not lumped circuit analysis.

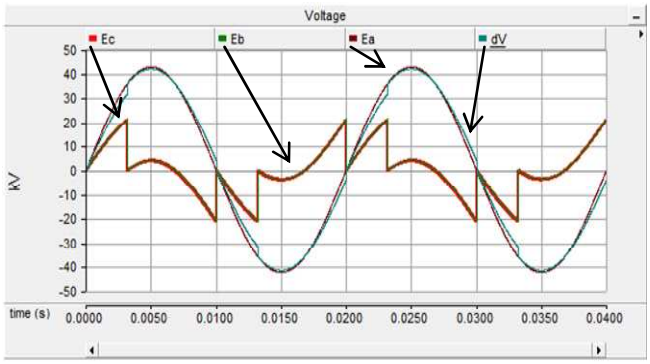

Fig 8. The potentials predicted for the model circuit of Fig. 3. The vertical scale for Eb and Ec has been increased by a factor of 5 for clarity, and these lines overlay each other. Ea is a clean sinusoidal wave, and dV deviates from a sinusoid when discharges occur.

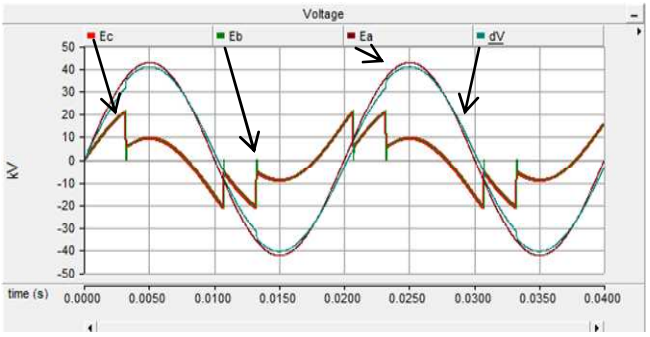

Fig 9. The model with a series resistor of 10 kΩ. The vertical scale for Eb and Ec has been increased by a factor of 5 for clarity, and these lines overlay each other. Ea is a clean sinusoidal wave, and dV deviates from a sinusoid when discharges occur.

III. Experimental Measurement of Induced Voltages

So that a situation similar to that encountered in the field could be created in the laboratory, a single overhead conductor was established 4.8 m from the ground. A small section of tower was erected within the same laboratory space. Fig. 10 shows this situation schematically in plan view. The faces of the tower are labeled N, E, S and W, not because these are the true compass bearings, but to establish relative directions.

As an object for testing, a 'stickman;' was devised and built. This provided person-like dimensions whilst being reproducible for modeling activities. Stickman is shown in Figure 11. This was constructed with 28 mm diameter copper tube. The 'shoe' capacitance was defined by using aluminum plates separated by 10 mm thick PMMA as shown in the detailed picture. The two feet combined to give a C_s of 200 pF. The test object was placed on the ground, at a number of locations at floor level.

A. *Verification of Voltage Measurement*

The voltage seen by the stickman was determined at 20 locations around the tower. The measurement was performed using a commercial high-impedance 1 GΩ probe attached to a DVM. However it was found that the high fields in which the measurements were performed led to systematic errors unless the HV probe and the instrument were both shielded by metallic boxes. In addition, the voltage divider and DVM were positioned inside the tower structure, and the associated cables kept as close to the ground as possible. The 1 GΩ impedance is in parallel with C_b and C_s changing the impedance division with C_a in Fig. 2. Assuming C_a is 1 pF this adds a systematic error into the measurement of -2% at 50 Hz. The error in the voltage measurement is ±5%.

To ensure the voltage measurement was correct, a small spark-gap was used for calibration. This is the ideal calibration technique given that the purpose of this measurement is to predict discharge across a gap. The breakdown voltage of two spheres with 1.275 cm diameter separated by 0.5 mm was determined by direct application of a voltage to the spheres. The voltages were measured with the same DVM and the associated HV probe. This experiment was repeated 6 times, each experiment recording 10 breakdown values in order to evaluate the mean value and the standard deviation [13]. The value of deviation should be less than 1% of mean value for satisfactory results. The sphere gap was then connected across one foot of the stickman, which was positioned 2 m from the south face of the tower, under the overhead line, in parallel with the 1 GΩ HV probe. As the overhead line voltage was increased the voltage rose accordingly, until reaching the breakdown point, where a visible and audible spark occurred causing a rapid drop in voltage. This breakdown test was repeated 10 times. In all these tests the corresponding overhead line voltage at breakdown was between 207-209 kV.

As the actual air density changes, the breakdown voltage values have to be corrected [13]. After correction, results gave the maximum difference between the mean value and standard deviation of data is 0.2% while the difference was 0.3% for

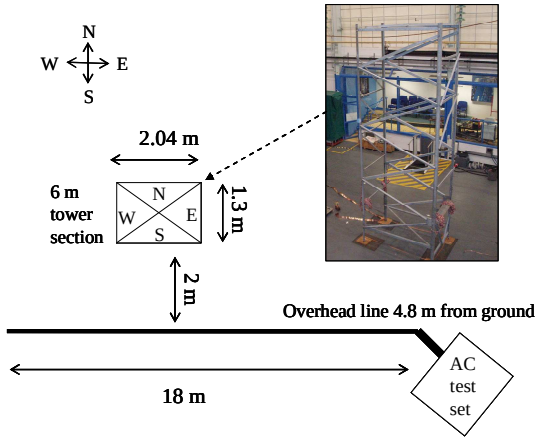

Fig. 10. A schematic plan of the large-scale experiment (not to scale). A photograph of the tower is also shown.

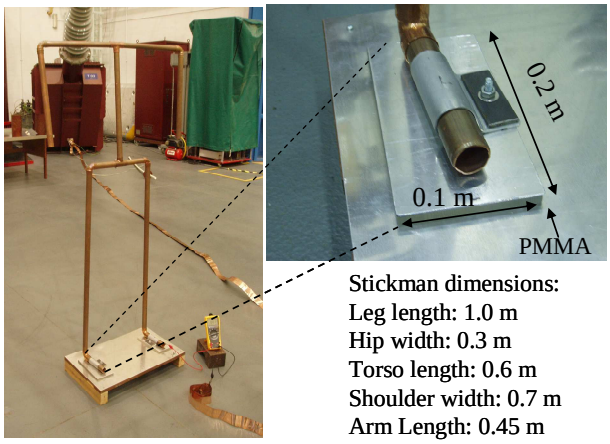

Fig. 11. The object used for testing; 'stickman'.

breakdowns recorded with a capacitively coupled stickman. Uncertainties in the breakdown measurements arose from the HV probe accuracy of ±5%, and an error of ±3% associated with the sphere gap voltage calibration method. This test has proven to be successful in validating the voltage measurements obtained via the HV probe and its associated DVM.

Finally, to ensure the 1 GΩ divider does not significantly change the voltage being measured, the voltage on the overhead line at which discharges occurred across the sphere gap was recorded 10 times with and without the divider in the circuit. The mean value of the overhead line voltage was 230 kV with the divider in the circuit compared to 215 kV without the divider. However, the presence of the voltage measurement equipment across the 16 MΩ stickman's shoe capacitance introduces a systematic error of 2%. Thus, the experimental setup measured stickman's potential with an accuracy of 5%.

B. *Induced Voltage Measurement in the Laboratory*

The voltage seen by the stickman was determined at the locations around the tower, 0.1, 0.5, 1.0, 1.5 and 2.0 m from each face of the tower. On the south-side of the tower the 2 m measurement was directly under the high voltage line. The data generated in these experiments is shown in Fig. 12.

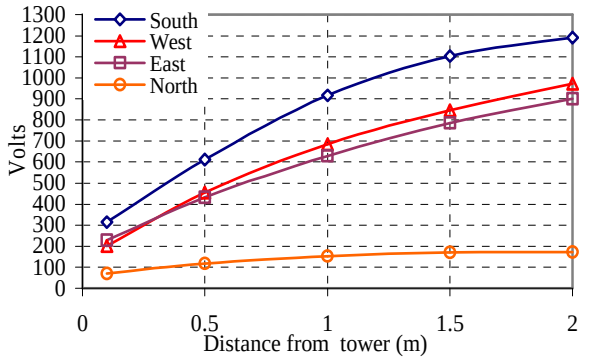

Fig. 12. Measurements of the voltage on stickman in the four directions defined by Fig.10. Polynomial lines of best fit are included.

IV. Measurement of AC Current Available

The maximum steady state ac current available was also measured. This was achieved by grounding one foot of the stickman through an ammeter. These measurements are shown in Fig. 13. This current is that which flows if good contact is made to ground and no arcing is present.

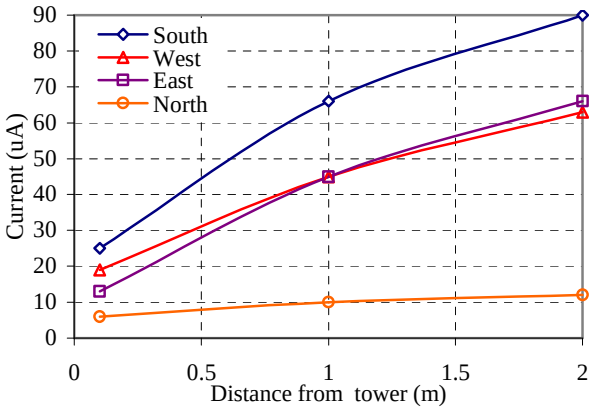

Fig. 13. Measurements of the current drawn through an earthed foot of stickman in the four directions defined by Fig. 10. Polynomial lines of best fit are included.

V. Predictions using CDEGS

The work reported here utilises the CDEGS sub package HIFREQ. The CDEGS package is based on a series of mathematical equations referring to both field theory and circuit analysis. The HIFREQ package can calculate current distributions for networks of overhead conductors and metallic grids. From the current distributions, HIFREQ calculates electric fields and scalar potentials in three dimensions [14].

The construction of the model is confined to building blocks of straight conductors (i.e. cylindrical physical shapes with a minimum length equivalent to their diameter). Thus the construction of a tower is time-consuming but simple. The representation of the stickman is also readily constructed. Within CDEGS, the towers are given the same frame dimensions but each metal bar is represented by a cylindrical conductor with the same diameter and resistivity.

Figs. 14 and 15 show the predictions of the software overlaid on the data presented in Figs. 12 and 13.

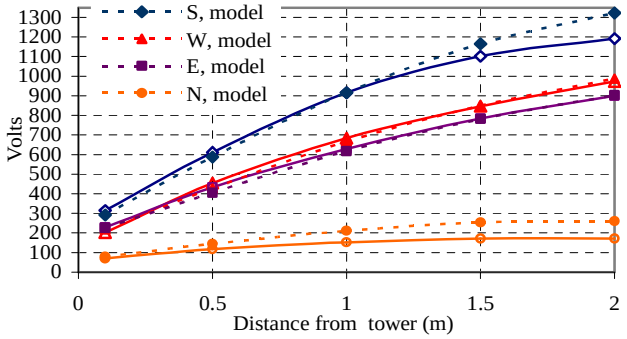

Fig. 14. Four lines showing the prediction by the software overlaid on the voltage measurements of Fig. 12. (Solid lines are measured voltages)

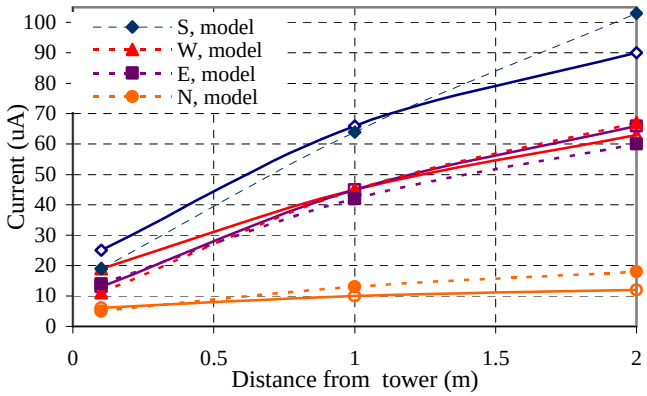

Fig. 15. Four lines showing the prediction by the software overlaid on the current measurements of Fig. 13. (Solid lines represent measured voltages)

VI. Discussion

The circuit models of discharge processes are consistent with the present understanding of the cause of microshocks. The reason for the development of multiple discharges per cycle is clear, and depends upon the instantaneous gap length and the induced voltage. The discharge current is controlled by the person's capacitance to ground. The series resistance controls the voltage to which the object collapses at discharge. This has been recorded as 500V in small scale laboratory tests on individuals [11], [12]. This may well be as result of skin impedance. Variation in this property with time may explain be responsible for the variability between people and occasions, and is worthy of further study.

CDEGS is a powerful tool to model the currents and voltages on objects close to overhead lines. The predictions of the software have been carefully compared to a simplified situation in the laboratory. The use of a single conductor and an object constructed from copper tube reduced the opportunity for uncertainties to arise between the measurement and the prediction. The measurement of voltage itself was complex because if precautions were not taken the voltage measurement method and the high field induced systematic errors in the voltage measurement. However these issues where overcome by careful routing of cables and shielding of devices. The method was successfully calibrated by use of sphere-sphere gaps.

Fig. 13 shows that the voltage predictions were accurate,

with differences of up to 10% between prediction and measurement where substantial voltages were measured. CDEGS generally predicted voltages higher than those measured, and in particular was highest in proportion directly underneath the HV line. Measured and predicted voltages were similar with less than a few percent difference on the eastern and western sides. The difference was much larger on the northern side where lower voltages were experienced due to shielding by the tower. Closer to the tower the predictions are more accurate.

The predictions by CDEGS of the current drawn to earth by the object were also found to be very accurate. Fig. 14 shows a maximum disparity of 13% in any location. On the Southern side of tower, closest to the overhead line conductor; a maximum 13% difference has been recorded between HIFREQ predictions and experimental current measurements with stickman positioned 2 m from tower. The maximum difference recorded on the eastern and western sides was 9%. HIFREQ has over-predicted the current on the northern side of tower where currents are very low due to shielding of the tower structure.

By use of the stickman it has been shown that the software tool CDEGS is capable of modeling the environment of stickman to with an accuracy of voltage and rms current of typically better than 10%. By improving the geometric model of stickman to better represent a human it is expected that CDEGS will provide a tool ideal for calculated exposure to microshocks on overhead lines. For most purposes using stickman in the model is expected to provide adequate accuracy for practical purposes of predicting harsh working environments which expose linesmen to risk of microshocks.

VII. Conclusion

Circuit models have been shown to be useful as an aid to understanding the microshocks process. The software package CDEGS has been shown to be capable of modeling a simplified situation equivalent to linesmen in proximity to overhead lines. These packages are capable of being developed into more sophisticated and readily accessible tools for modeling practical situations in which microshocks occur.

As a result of this work, CDEGS will be used to develop more realistic models of linesmen. These will be developed in the context of real working environments so the results can be compared to controlled practical working conditions. Most importantly these models can now be expected to predict conditions in which microshocks can occur, help avoid difficult working environments, and develop mitigation techniques.

VIII. References

[1] J. P. Reilly and L. R. Delapace, "Electric and magnetic field coupling from high voltage ac power transmission lines - Classification of short-term effects on people," *IEEE Transactions on Power Apparatus and Systems*, vol. PAS-97, pp. 2243-2252, 1978.

[2] *IEEE standard for safety levels with respect to human exposure to electromagnetic fields, 0-3 kHz*, IEEE Standard C95.6-2002.

[3] T. Bracken, R. Senior, and M. Tuominen, "Evaluating Occupational 60-Hz electric field exposures for guideline compliance," *Journal of Occupational and Environmental Hygiene*, vol. 1, pp. 672 - 679, 2004.

[4] T. Bracken, "Assessing compliance with power frequency magnetic field guidelines," *Health Physics Society*, vol. 83, pp. 409 - 416, 2002.

[5] R. J. Liedtke, "Fundamentals of Bioelectrical Impedance Analysis," 1988, [online] Available: www.rjlsystems.com.

[6] C. F. Dalziel, "Electric shock hazard," *IEEE spectrum*, 1972, pp. 41-50

[7] W. Zhancheng, H. Jiusheng, and L. Shanghe, "Measurements of Body Impedance for Esd," *Electrical Overstress/Electrostqtic Discharge Symposium*, pp. 132 - 134, 1997

[8] *Effects of current on human beings and livestock*, International Electrotechnical Commission IEC/TS 60479-3, 1999.

[9] H. Kanai, I. Chatterjee, and O. P. Gandhi, "Human Body Impedance for Electromagnetic Hazard Analysis in the VLF to MF Band," *IEEE Transactions on Microwave Theory and Techniques,*, vol. 32, pp. 763, 1984.

[10] J. P. Reilly and W. D. Larkin, "Human sensitivity to electric shock induced by power-frequency electric fields," *IEEE Transactions on Electromagnetic Compatibility*, vol. EMC-29, pp. 221-232, 1987.

[11] J. P. Reilly and W. D. Larkin, "Electrocutaneous stimulation with high voltage capacitive discharges," *IEEE Transations Biomedical Engineering*, vol. BME-30, pp. 631-641, 1983.

[12] J. Reilly, W. Larkin, R. Taylor, and V. Freeman, "Human reactions to transient electric currents - Annual report," Johns Hopkins Univ. Appl. Phys. Lab., Laurel, MD, Rep. CPE-8203, July 1982.

[13] E. Kuffel, E., W. S. Zaengl. And J Kuffel, (2000) *High Voltage Engineering: Fundamentals*, Second edition, Newnes, 2000 pp. 78-89

[14] Safe Engineering Services & Technologies, "*Hifreq user's manual*", [Online document], [cited 2006 Jan 30], Available HTTP: http://www.sestech.com/common/manual/engineering/hifreq.pdf

IX. Biographies

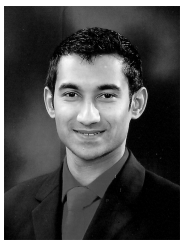

Aruna Gunatilake was born in Bogawanthalawa, Sri Lanka. He completed his BSc in Electrical Engineering at the University of Moratuwa, Sri Lanka and his MPhil at UMIST, Manchester. He is a student member of the IET, IEEE and IEEE Power Electronics society. He worked for two years as a software developer and as an international workshop coordinator in a leading Pharmaceutical organization in Denmark before he joined UMIST. Since 2004 he has been a PhD student in the School of Electrical and Electronic Engineering in The University of Manchester.

Yasir Ahmed (M'07) was born in Edinburgh, Scotland. He received a BEng (Hons) in Electrical Engineering from Sudan University of Science and Technology in 1998 and an MSc in Communication Systems and Signal Processing from University of Bristol in 2000. He worked in research and development for Celestica (UK) between 2000 and 2004. He is currently an Engineering Doctorate (EngD) research student at the Electrical Energy and Power Systems Group of the School of Electrical and Electronic Engineering at the University of Manchester. He is a Member of the Institution of Engineering and Technology.

Simon M. Rowland (SM'07) was born in West Ham, London, England. He completed his BSc in Physics at The University of East Anglia and his PhD at London University. Dr. Rowland was awarded the IEE Duddell premium in 1994 and became a Fellow of the IET in 2000. He has worked in industrial research on dielectric materials and their applications, and held senior management posts in manufacturing organisations. Since 2003 he has been a Senior Lecturer in the School of Electrical and Electronic Engineering in The University of Manchester.